Food Chemistry 383 (2022) 132387

Contents lists available at ScienceDirect

Food Chemistry

journal homepage: www.elsevier.com/locate/foodchem

Enzyme-extracted raspberry pectin exhibits a high-branched structure and enhanced anti-inflammatory properties than hot acid-extracted pectin

Dongmei Wu [a], Shiguo Chen [a,b], Xingqian Ye [a,b], Xiaoliang Zheng [c], Shokouh Ahmadi [a], Weiwei Hu [a], Chengxiao Yu [a], Huan Cheng [a], Robert J. Linhardt [d], Jianle Chen [a,*]

[a] College of Biosystems Engineering and Food Science, Ningbo Research Institute, National-Local Joint Engineering Laboratory of Intelligent Food Technology and Equipment, Zhejiang Key Laboratory for Agro-Food Processing, Integrated Research Base of Southern Fruit and Vegetable Preservation Technology, Zhejiang International Scientific and Technological Cooperation Base of Health Food Manufacturing and Quality Control, Zhejiang University, Hangzhou 310058, China
[b] Zhejiang University Zhongyuan Institute, Zhengzhou 450000, China
[c] Center for Molecular Medicine, Hangzhou Medical College, Hangzhou 310013, China
[d] Center for Biotechnology & Interdisciplinary Studies, Department of Chemistry & Chemical Biology, Rensselaer Polytechnic Institute, Biotechnology Center 4005, Troy, NY 12180, USA

ARTICLE INFO

Keywords:
Raspberry
Polysaccharide
Arabinan sidechains
Purification
Characterization
Immunomodulatory

ABSTRACT

To characterize the structure of purified raspberry pectin and discuss the impact of different extraction methods on the pectin structure, raspberry pectin was extracted by hot-acid and enzyme method and purified by stepwise ethanol precipitation and ion-exchange chromatography isolation. Enzyme-extracted raspberry pectin (RPE50%-3) presented relatively intact structure with molecular weight of 5×10^4 g/mol and the degree of methylation was 39%. The 1D/2D NMR analysis demonstrated RPE50%-3 was a high-branched pectin mainly containing 50% homogalacturonan, 16% branched α-1,5-arabinan and α-1,3-arabinan, 18% β-1,4-galactan and β-1,6-galactan. Acid-extracted raspberry pectin (RPA50%-3) contained less arabinan than RPE50%-3. Moreover, RPE50%-3 inhibited the nitric oxide (NO), TNF-α, IL-6 production of lipopolysaccharide-induced macrophages by 67%, 22% and 46% at the dosage of 200 ug/mL, while the inhibitory rate of RPA50%-3 were 33%, 9%, and 1%, respectively. These results suggested that enzyme-extracted raspberry pectin contained more arabinan sidechains and exhibited better immunomodulatory effect.

1. Introduction

Raspberry (*Rubus idaeus L.*), as one member of the berry family, is a fine fruit widely distributed and consumed in different climatic and soil regions of Europe, North America, South Africa and Asia (including Northeast China), which possesses delicious taste and high nutritional and medicinal value (Yu et al., 2015). According to Food and Agriculture Organization (FAO) data, with the great economic importance in berry fruit, the global production of raspberry has increased around 46% from 373 thousand tons in 2010 to 684 thousand tons in 2019. Raspberry is known as a valuable source of phenolic compounds. However, in recent years, many food scientists and nutritionists have begun to pay attention to the functional polysaccharides in raspberries, which have been reported to possess anti-tumor activity (Yang, Xu, & Suo, 2015), immune regulation (Tian, Yang, Wu, & Chen, 2020), antioxidative and anti-glycation activity (Chen et al., 2020; Xu et al., 2019).

Pectin is an acid heteropolysaccharide existing widely in the plant cell wall of fruits and vegetables, and it is popular in scientific fields due to its health-promoting functionality (Wu et al., 2020a; Wu et al., 2020b). As one of the most structurally complex polysaccharides, pectin mainly consists of three domains: homogalacturonans (HG), type I of rhamnogalacturonan (RG-I), and type II of rhamnogalacturonan (RG-II) (Mohnen 2008). Additionally, different extraction methods lead to different structural characteristics (Voragen, Coenen, Verhoef, & Schols, 2009). The commercial pectin products usually were obtained from citrus peel and apple pomace by harsh acid extraction. However, some studies have reported that hot acid extraction can induce the degradation of neutral sidechains in citrus pectin (Chen et al., 2021; Zhang et al., 2018). Recently, ultrasound, monosonication, and hot-compressed water have been researched for the pectin extraction. Shivamathi et al. (2022) have reported that ultrasound-assisted extraction can increase the pectin yield. Also, at the condition of 42 °C and pH12,

* Corresponding author.
E-mail address: chenjianle@zju.edu.cn (J. Chen).

https://doi.org/10.1016/j.foodchem.2022.132387
Received 6 November 2021; Received in revised form 11 January 2022; Accepted 6 February 2022
Available online 9 February 2022

monosonication could accelerate the extraction of citrus RG-I pectin and the maximum yield was 25.51% (Hu, Ye, Chantapakul, Chen, & Zheng, 2020). However, all of these sonication treatment and high temperature can induce poor uniformity of pectin product and the destruction of pectin microstructure, especially the neutral sidechains (Hu, Ye, Chantapakul, Chen, & Zheng, 2020; Mao et al., 2019). Enzyme extraction is a very mild method for pectin extraction. The most commonly used enzymes include cellulase, hemicellulase, protease, and pectinesterase. The combination of these enzymes could accelerate the cleavage of cell wall structure, so as to release pectin. Cui et al. (2020) have studied the effects of different extraction methods on the structure and fermentation characteristics of citrus pectin and they found that cellulase-extracted pectin possessed more extended conformation and was more beneficial for the growth of intestinal microorganisms. Milošević and Antov (2022) showed that compared to acid extraction, cellulase-xylanase-extracted pectin had higher molecular weight, more uronic acid, lower starch content and better antioxidant ability than acid-extracted pectin. Pectin is the major component of the soluble fiber in raspberry. Yu et al. (2015) have used the complex enzymes (cellulase, pectinase, and papain) to extract the polysaccharides from raspberry fruits, but pectinase did destroy the structure of pectin. Chen et al. (2020) and Xu et al. (2019) have reported the antioxidant activities of crude raspberry pectic polysaccharides extracted by acid or hot water. However, the fine structural characteristics of pure raspberry pectin remains unclear. Additionally, there has been no systematic evaluation of the effects of different extraction methods on the structure and functionality of pure raspberry pectin.

Dietary pectins are considered as immunological molecules in some immune diseases, such as IBD, due to direct or indirect effects on immune system (Mzoughi et al., 2018; Wu et al., 2021b). It has been reported that citrus pectin can interact with the Toll-like receptors (TLRs) in macrophages and, thus, regulate the immune responses in colitis and ileitis mice (Ishisono et al., 2019; Sahasrabudhe et al., 2018). Recently, numerous studies focused on the structure–activity relationship of pectin regulating inflammation (Wu et al., 2021c). Low degree of methylation contributes to the pectin function on alleviating the gut inflammation (Fan et al., 2020; Wu et al., 2021a). Pectin with high amount of neutral sidechains could directly interact with macrophages and inhibit IL-6 production, while no marked reduction was observed in the culture of citrus pectin, which contained less sidechains (Ishisono et al., 2019). Therefore, the immunomodulatory activity of pectin is highly structure-dependent. Macrophages are important immune cells involved in the initiation of inflammation and lipo-polysaccharides (LPS)-induced macrophages will secrete more pro-inflammatory mediators, such as inflammatory cytokines (IL-6, IL-1β, and TNF-α), nitric oxide (NO) and reactive oxygen species (ROS). However, the effects of purified raspberry pectin on inflammatory macrophages remain unclear and whether pectins extracted by different methods can induce different immune responses in immune cells need to be studied.

Therefore, our hypothesis is that different extraction methods will lead to different structure and bioactivity of raspberry pectin. In this study, crude raspberry polysaccharides were extracted by the hot acid extraction and enzyme extraction to compare the effects of vigorous extraction method and mild extraction method on the structure and activity of pure raspberry pectin. Stepwise ethanolic precipitation and ion-exchange chromatography column were combined to purify and obtain the pure pectin fraction. The structural characterization of pure raspberry pectin was performed, and its immunomodulatory activity was evaluated. Our results afford fine structural information for raspberry pectin and also provides insights on efficient extraction of the functional pectin in the food industry.

2. Materials and methods

2.1. Materials

Raspberry fruits purchased from the local market in Hangzhou, China were used for pectin extraction. Freeze-dried fruits were thoroughly ground into fine powder (200-mesh sieve), soaked in absolute ethanol with stirring, oven-dried, and then kept in desiccators for subsequent extraction and analysis. Commercial pectin, monosaccharide standards, D_2O and other chemicals of analytical grade were all purchased from Sigma-Aldrich (Shanghai, China). RAW264.7 cell lines were kindly provided by Dr. Xiao-liang Zheng (Center for Molecular Medicine, Zhejiang Academy of Medical Sciences, Hangzhou, China). RPMI 1640 medium, fetal bovine serum (FBS) and the 3-(4,5-dimethythiazol-2-yl)-2,5-diphenyltetrazolium bromide (MTT) were obtained from Sigma-Aldrich (Shanghai, China).

2.2. Pectin extraction under different methods

Conventional hot acid extraction according to Kurita, Fujiwara, and Yamazaki (2008): Dried fruit powder was dispersed in HCl solution with a pH value of 1.5 (solid–liquid ratio of 1:40, w/v). The suspensions were stirred and heated at 85 °C for 1 h. After extraction, the resulting slurries were cooled to room temperature (23 °C), neutralized to pH 7.0, filtered using a 400-mesh filter bag, and centrifuged (8000 × g, 10 min) to separate some insoluble cell wall components like cellulose and hemicelluloses in the sediment from pectic polysaccharides soluble in the HCl solution. The supernatant was then collected and prepared for stepwise ethanol precipitation.

Enzyme extraction according to Yu et al. (2015) with minor modifications: In brief, raspberry fruit powder was added to 500 mL citric acid buffer liquid (pH 5.0) mixed with 1 g of cellulase (Sigma-Aldrich, Shanghai, China) and 20 mg of papain. This enzyme extraction was carried out at 55 °C under stirring for 5 h. After that, the temperature was reduced to 37 °C, and 0.5 mL α-amylase and 0.1 mL glucoamylase were added, which can hydrolyze starch into glucose. These enzymolysis reactions was kept for 3 h. The solution was then heated at 100 °C for 5 min to inactivate the enzyme. The following steps were the same as that of acidic extraction.

2.3. Stepwise ethanolic precipitation of crude pectic polysaccharides

Fig. S1 shows the scheme for precipitation of the crude raspberry extract, according to Guo et al. (2016) with some modifications.

Ethanol (125 mL) was gradually added to a 500 mL acidic extract under stirring to reach a final ethanol concentration of 20%. A constant flow pump was used to control the flow rate of ethanol addition at 11 mL/min. After standing at 4 °C for 4 h, the precipitates were collected via centrifugation (8000 × g, 10 min) and washed three times with 95% ethanol. The sediment was dissolved, dialyzed, and lyophilized to obtain RPA20%. Different volumes of ethanol were stepwise pumped into the supernatant to obtain the concentration of 30%, 40%, 50%, 60% and 70%. And the precipitated fractions RPA30%, RPA40%, RPA50%, RPA60% and RPA70% were collected, respectively, as described above.

The enzymatic aqueous extract was only precipitated with 30%, 50% and 70% ethanol, and RPE30%, RPE50%, RPE70% was obtained for further determination.

2.4. Fractionation of pectic polysaccharides by Q-fast flow column (QFF) chromatography

QFF column chromatography was applied to isolate the crude raspberry fiber as previously described (Liu et al., 2020). RPA50% or RPE50% (150 mg) were dissolved in 10 mL of distilled water and then applied to a QFF column (3 × 27 cm). Elution was performed by a linear gradient of 0–0.5 M sodium chloride solution at a flow rate of 0.5 mL/

min. Every tube of 4 mL solution was collected. The content of carbohydrate fractions was determined by the improved phenol–sulfuric acid method at 490 nm. Fractions within one peak referring to the same fraction were pooled, dialyzed, and then lyophilized.

2.5. Chemical composition determination of different polysaccharide fractions

The total amount of carbohydrates was analyzed according to the phenol–sulfuric acid (Soria et al., 2010). The total phenolic content of the pectic fraction was analyzed using the Folin-Ciocalteu method (Kazemi, Khodaiyan, & Hosseini, 2019).

The degree of methylation (DM) was determined by the m-phenylphenol method (Levigne, Thomas, Ralet, Quemener, & Thibault, 2002). After saponification, the pectin solution was prepared to analyzed methanol and acetic acid using high-performance liquid chromatography (HPLC) (Waters 1525, US) equipped with a C18 column (Sino-Chrom ODS-BP 250 mm × 4.6 mm, 5 mm, Elite, China) and a refractive index (RI) detection (Waters 2414, US). Isopropanol was used as internal standard and 4 mM sulfuric acid was the mobile phase.

2.6. Assessment of molecular weights

The homogeneity and molecular weight of pectin were analyzed by high-performance (HP) size exclusion chromatography (*SEC*) with a multi-angle laser light scattering (MALLs) (Wei et al., 2019).

2.7. Determination of monosaccharide composition

The monosaccharide composition was determined by a HPAEC-PAD method (Hu, Ye, Chantapakul, Chen, & Zheng, 2020). Pectins (~2 mg/mL) were decomposed by 4 M trifluoroacetic acid (TFA) at 110 °C for 8 h. The hydrolysates were evaporated with 200 μL methanol under nitrogen blower twice, and then diluted to 10 mL with deionized water. After filtered through a membrane of 0.22 μm, 25 μL sample solution was injected into the ICS-5000 system (Thermo Fisher, USA) coupled with a Carbopac-PA10 analytical column (4 mm × 250 mm, Thermo Fisher, USA) and an electrochemical detector. The column was washed with 18 mM NaOH for 15 min, followed by a 35 min elution with a fixed 18 mM NaOH in 100 mM sodium acetate. The flow rate was set at 1 mL/min, and all fractions were analyzed at 30 °C.

2.8. Determination of FT-IR spectra

FT-IR spectra of pectins were detected through a Fourier-transform infrared spectrophotometer (Nexus IS10 FTIR, Thermo Nicolet, USA) (Zhang et al., 2018). Pectins (~2 mg) were ground together with KBr powder and pressed into pellets for FT-IR scanning in the range of 4000–400 cm^{-1}.

2.9. Cell culture conditions and cytotoxicity assay of RAW264.7 cell line

The cell culture methods were according to Yang et al (2018). Murine macrophages RAW264.7 cells were cultured in RPMI-1640 medium containing 10% FBS and 2.5% antibiotic and incubated at 37 °C in a 5% CO_2 humidified atmosphere. The cytotoxicity of the pectins was performed by a commercial cell counting kit-8 (CCK8) (Solarbio Life Science, Beijing, China). RAW264.7 cells (2×10^5 cell/well) were seeded into 96 well plate and incubated with various concentrations (50 μg/mL, 100 μg/mL, 200 μg/mL, 400 μg/mL, and 800 μg/mL) of the samples for 24 h. At the end of the incubation period, 10 μL of CCK8 buffer solution was added to each well and the culture plate was incubated at 37 °C for 2 h. Subsequently, the absorbance of all the wells was measured at 450 nm using a microplate reader (Bio-Rad, USA).

2.10. Determination of NO release of RAW264.7 cell culture

The content of released NO from active RAW 264.7 cells induced by LPS was determined by NO assay kit (Beyotime Technology, Shanghai, China). Cells were plated and incubated with different pectic fractions at different concentrations and LPS (5 μg/mL) for 24 h. After incubation, the culture supernatants were collected and the NO content was analyzed according to the instructions.

2.11. Measurement of ROS of RAW264.7 cell culture

The determination of ROS generation of RAW 264.7 cells after pectins or LPS treatment was performed using the commercial kit (Beyotime Bio-Technology, Shanghai, China). LPS-induced RAW 264.7 cells were incubated by the pectic samples at different concentrations (50 μg/mL, 100 μg/mL, 200 μg/mL, 400 μg/mL, and 800 μg/mL) for 24 h. DCFH-DA (100 μL) was then diluted in the medium and added to each well and incubated for another 30 min. The cells were washed three times with PBS solution and covered with 100 μL of fresh medium. The intracellular ROS levels were measured using a fluorescence microplate reader (SpectraMax® iD5, Molecular Devices, Shanghai, China) with an excitation wavelength at 485 nm and an emission wavelength at 525 nm.

2.12. Measurement of TNF-α, IL-6, and IL-1β in RAW 264.7 cell culture

The level of pro-inflammatory cytokines was according to previous study (Wu et al., 2021c). The concentration of IL-6, IL-1β, and TNF-α were measured using immunoenzymatic assay (ELISA) kits (mlbio Biotechnology, Shanghai, China), according to the manufacturer's protocol.

2.13. Structure characterization of RPE50%-3

2.13.1. Determination of NMR spectra

RPE50%-3 (15 ~ 20 mg) was dissolved in D_2O and lyophilized twice, and then dissolved in D_2O and placed in an NMR tube. The ^1H NMR, ^{13}C NMR, ^1H–^1H COSY and ^1H–^{13}C HSQC were detected on an Agilent DD2-600 MHz spectrometer (Agilent Technologies, Santa Clara, CA, USA) (Wei et al., 2019). The resonances of $–CH_3$ groups of acetone in D_2O were used as the internal reference.

3. Results and discussion

3.1. Analysis of ethanol-precipitated fractions from acid-extracted raspberry polysaccharide (RPA) and enzyme-extracted raspberry polysaccharide (RPE)

According to the procedure shown in Fig. S1, six fractions RPA20%, RPA30%, RPA40%, RPA50%, RPA60%, and RPA70% were collected. The ratio and basic chemical compositions were listed in Table 1. The content of RPA50% was 74%, suggesting RPA50% was the major fraction of acid-extracted polysaccharides. From the results of monosaccharide composition and molecular weight (M_w), RPA20% and RPA30% were mainly composed of glucose, xylose, galactose (Gal), arabinose (Ara) and galacturonic acid (GalA), indicating the presence of many hemicellulose with a huge M_w. The monosaccharide composition of RPA40% was similar to that of RPA50%. The high amount of GalA, arabinose, galactose and glucose suggested the presence of pectic substances and some xyloglucan (Fig. S2), and the content of GalA in RPA40% and RPA50% was higher than other fractions, indicating that pectin mainly existed in RPA40% and RPA50%. While the M_w of RPA40% was larger than that of RPA50%, suggesting that stepwise ethanol precipitation could isolate similar polysaccharides with different molecular weight. The last two minor fractions RPA60% and RPA70% contained more than 50% of arabinose and galactose, suggesting the small M_w fraction of acid-extracted products mainly

Table 1
Chemical composition and molecular properties of RPA fractions and RPE fractions.

	Monosaccharide compositions (mol%)							Yield (%)	Phenol (mg/g)	M_w (KDa)	Polydispersity
	Arabinose	Galactose	Rhamnose	Galacturonic acid	Glucose	Xylose	Mannose				
RPA20%	12.57 ± 0.21	21.76 ± 0.07	1.81 ± 0.06	10.46 ± 2.52	35.91 ± 2.3	17.47 ± 0.08	–	0.5 ± 0.01	89 ± 0.9	200 ± 0.21	2.03 ± 0.36
RPA30%	11.48 ± 1.28	19.18 ± 2.91	1.86 ± 0.67	11.84 ± 0.97	50.08 ± 2.5	5.57 ± 1.34	–	0.2 ± 0.00	92 ± 1.2	250 ± 0.11	2.52 ± 0.81
RPA40%	8.24 ± 0.98	26.91 ± 1.00	4.32 ± 0.62	43.30 ± 4.32	13.96 ± 1.7	3.28 ± 0.03	–	1.3 ± 0.07	60 ± 0.5	262 ± 0.45	2.62 ± 0.45
RPA50%	9.96 ± 0.27	28.09 ± 0.72	4.86 ± 0.46	43.26 ± 2.42	10.53 ± 1.1	3.31 ± 0.13	–	11.6 ± 0.3	49 ± 0.7	154 ± 0.12	4.63 ± 1.13
RPA60%	16.59 ± 0.09	46.26 ± 1.12	7.68 ± 0.17	11.15 ± 1.54	13.35 ± 1.3	4.98 ± 1.50	–	0.6 ± 0.03	20 ± 0.8	65 ~ 9	2.40 ± 0.02
RPA70%	18.22 ± 0.11	37.57 ± 0.79	9.66 ± 0.21	6.62 ± 0.73	24.12 ± 0.5	4.74 ± 0.09	–	1.4 ± 0.05	29 ± 1.4	70 ~ 17	2.07 ± 0.07
RPE30%	15.31 ± 0.49	10.18 ± 0.31	3.69 ± 0.47	7.32 ± 0.18	46.02 ± 2.17	9.91 ± 0.77	7.24 ± 0.06	2.0 ± 0.02	32 ± 0.9	11790 ± 0.56	5.81 ± 0.03
RPE50%	14.50 ± 0.1	11.60 ± 0.01	6.79 ± 0.49	40.77 ± 3.18	16.97 ± 0.03	4.28 ± 0.21	5.28 ± 0.34	13.2 ± 0.21	23 ± 0.7	265 ± 1.18	6.02 ± 0.94
RPE70%	5.01 ± 0.24	7.20 ± 2.39	3.55 ± 0.24	3.87 ± 1.77	55.79 ± 2.3	10.73 ± 1.37	11.71 ± 0.8	4.2 ± 0.13	19 ± 0.2	122 ± 1.14	2.13 ± 0.54

Values represent means ± standard derivatives of three replicates;
- indicated not detected.

consisted of neutral sidechains and hot acid extraction might lead to the severe degradation of neutral sidechains of pectin. These results suggested that one-step ethanol precipitation (ratio of 3:1 ethanol/water) generally led to complex polysaccharides of multiple components and pectic polysaccharides mainly consisted in RPA50%. Moreover, RPA60% and RPA70% are composed of two polysaccharide fractions and with concentrations inversely proportional to the volume of ethanol (Fig. 1A). The smaller M_w fraction dominated in RPA70%, also revealing that ethanol solution of high concentration helps to precipitate out small molecules (Hu & Goff 2018). The major polysaccharides of large M_w could be collected by 50% ethanol precipitation. The low polydispersity index (M_w/M_n, close to 1) demonstrates homogeneous polysaccharide fraction (Wang, Liu, & Qin, 2017). According to the gel permeation chromatography (GPC) profile, all of the values of polydispersity fall in the range of 2.03 ~ 4.63 (Table 1), suggesting that fractions obtained by ethanol precipitation were polydisperse aggregates, and further purification were needed to isolate the pure pectin from RPA50%.

Raspberry was also viewed as a rich source of phenol compounds, which could interact with polysaccharides (Liu, Le Bourvellec, & Renard, 2020), so the phenol content of each fraction was determined. The RPA20% ~ RPA50% contained much higher amount of phenols (89 mg/g, 92 mg/g, 60 mg/g, and 49 mg/g, respectively) than RPA60% and RPA70%, suggesting that raspberry phenol compounds tended to interact with large M_w polysaccharides.

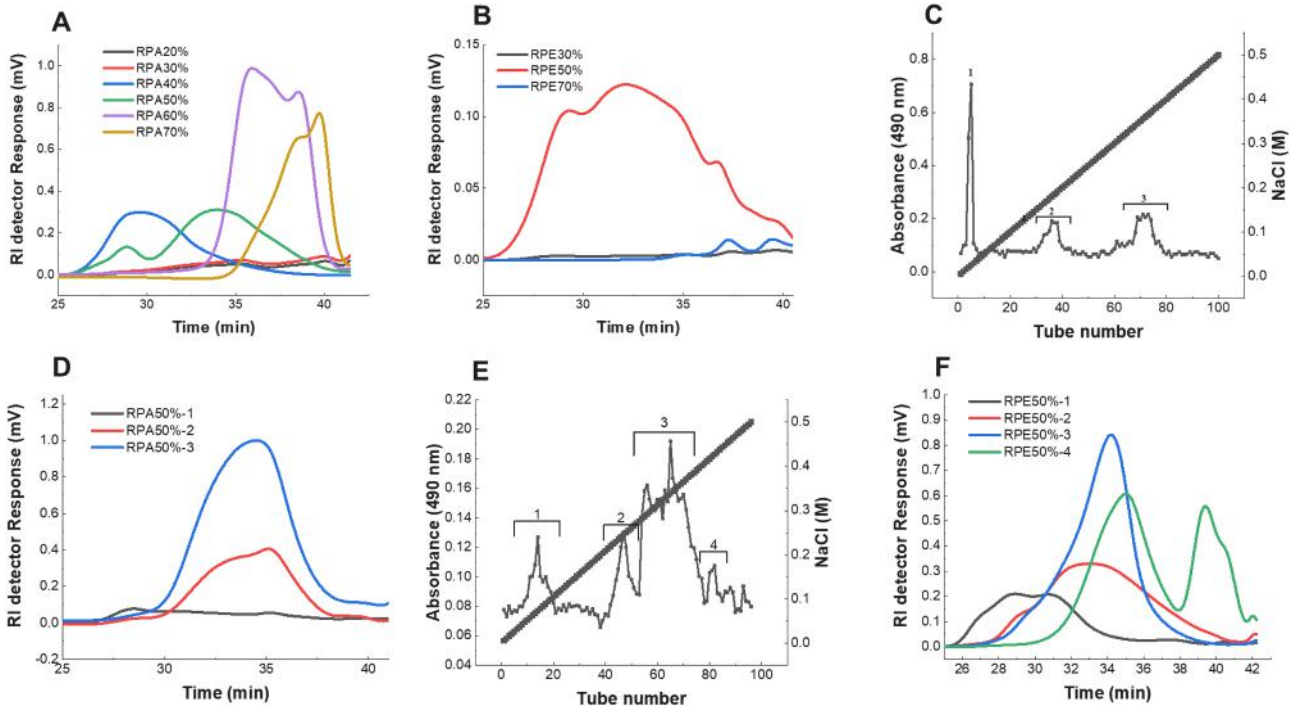

Fig. 1. Stepwise ethanolic precipitation and QFF column isolation of RPA and RPE: (A) HPGPC profiles of RPA fractions (B) HPGPC profiles of RPE fractions (C) Elution profile on QFF column of RPA50% (D) HPGPC profiles of RPA50% fractions (E) Elution profile on QFF column of RPE50% (F) HPGPC profiles of RPE50% fractions.

The RPE supernatant was also applied to gradient precipitation by 30%, 50% and 70% ethanol concentration, as shown in Fig. S1. The chemical composition and molecular properties of RPE fractions were presented in Table 1. Compared to RPA fractions, all of the RPE fractions represented relatively larger M_w, suggesting that enzyme extraction could afford large molecules. The high amount of glucose in all these fractions indicating that many hemicellulose with different M_w might be released by cellulase (Laroze, Soto, & Zúñiga 2010). Compared to RPA fractions, all of the RPE fractions contained relatively higher amount of glucose. This might be due to the release of soluble glucan and the activities of α-amylase and glucoamylase, which hydrolyzed starch into dextrin of small M_w precipitating with other polysaccharides fraction. RPE30% mainly consisted of glucose, xylose, arabinose, galactose, which was similar to RPA20% and RPA30%. Additionally, some mannose existed in RPE30%, suggested the mannan or glucomannan (hemicellulose) might be released from the interaction with insoluble cellulose. It has been reported that hemicellulose could coat the cellulose microfibrils via hydrogen bonding and van der Waals interactions (Cosgrove 2014; Gu & Catchmark, 2013). The content of GalA in RPE50% was about 41%, indicating that pectic substances mainly existed in RPE50%. RPE70% contained almost 80% glucose, and the amount of neutral sidechain (galactan and arabinan) was much lower than that of RPA70%, indicating that the small M_w fraction of enzyme-extracted products mainly contained glucan and enzyme extraction could degrade cellulose or hemicellulose into relatively low M_w glucan without degradation of arabinan and galactan. Moreover, the supernatant from 70%-ethanol-precipitation of RPA contained much more arabinose than that of 70%-ethanol-precipitation of RPE (Fig. S4). Moreover, the proportion of galactose in RPA20%~RPA70% fractions was about two or three times that of Ara, while in RPE30%~RPE70% fractions, the ratio of arabinose was similar as that of galactose. These results confirmed the degradation of arabinan sidechains induced by hot-acid extraction (Chen et al., 2021). RPE70% mainly consisted of water-soluble glucan, while RPA60% and RPA70% contained higher amount of galactose, arabinose, rhamnose and GalA, suggesting that hot-acid extraction might also lead to the rupture of RG-I main chain and the degradation of arabinogalactan. The results of phenol content (Table 1) revealed that enzyme-extracted fractions contained less phenol compounds than acid-extracted fractions, suggesting that enzyme combinations might help break the interactions between phenols and polysaccharides. The M_w of the RPE fractions were also determined by HPSEC-MALLs. As shown in Table 1, the decreasing order of M_w of RPE fractions was similar to that of RPAs. RPE30% was of huge M_w and RPE70% mainly contained low-M_w polysaccharides. RPE50% with high polydispersity, mainly containing pectic substances, was used for further purification of raspberry pectin by the QFF column.

3.2. Analysis of pure pectins obtained by QFF gradient elution

Crude polysaccharides RPA50% was then fractionated by anion exchange chromatography on the QFF column, and the eluted solution was collected by a fraction collector. The total sugar content in every tube was determined. As shown in Fig. 1C, three major peaks of polysaccharides were eluted from RPA50%. As listed in Table 2, the presence of neutral hemicellulose with high molecular weight dominated the earlier eluting fraction (RPA50%-1). Negatively-charged fractions, eluted in the gradient of NaCl solution, were obtained and noted as RPA50%-2 and RPA50%-3. The polydispersity of these three fractions were 2.36, 1.37 and 1.23, respectively. RPA50%-2 contained 18% of GalA and other neutral fractions, suggesting the mixture of polysaccharides. RPA50%-3, the major component of RPA50%, contained 66% of GalA. The one peak in the GPC profile revealed that RPA50%-3 was the purified pectin under hot acid extraction, with a molecular weight of 77 kDa.

RPE50% was applied to the QFF column for further purification of enzyme-extracted pectin. As shown in Table 2 and Fig. S6, four fractions (RPE50%-1, RPE50%-2, RPE50%-3 and RPE50%-4) were eluted in increasing order of GalA content. The polydispersity values were 1.59, 3.02, 1.97 and 2.92, respectively. Neutral fractions mainly contained glucans of large M_w in RPE50%-1 and RPE50%-2. RPE50%-3 was the major fraction with a ratio of 69%, in the form of pure RG-I pectin with M_w of 51 kDa, containing more neutral sidechains than RPA50%-3, especially more arabinose. These results confirmed that acid extraction induced the degradation of arabinan sidechains in RG-I pectin. RPE50%-4 mainly contained the HG pectin of low M_w, which might crosslink with cellulose or hemicellulose in the cell wall polysaccharide network and could be released by cellulase (Zykwinska, Ralet, Garnier, & Thibault, 2005).

We examined the FT-IR spectra of the pectins to determine the structural characteristics and differences between RPA50%-3 and RPE50%-3. The IR spectra of RPA50%-3 and RPE50%-3 were essentially identical (Fig. S3). The strong absorption band observed at 3447 cm^{-1} represented O—H stretching, and the weak band at approximately 2923 cm^{-1} was attributed to the C—H stretching of polysaccharides. The wide, intense bands at 1621 cm^{-1} originated from the stretching vibrations of carboxylate ion (COO^-) moieties. The low absorption band at 1747 cm^{-1} corresponded to the C═O stretching of methyl-esterified carboxylic groups (Vriesmann & de Oliveira Petkowicz 2009), indicating the low DM of both RPA50%-3 and RPE50%-3. The presence of GalA was also confirmed by the apparent absorption band at 1417 cm^{-1} (Saberian, Hamidi-Esfahani, Gavlighi, & Barzegar, 2017). Moreover, the absorption bands at 1239 cm^{-1} demonstrated the C—O stretching of pectin (Szymanska-Chargot & Zdunek, 2013). These data indicated both RPA50%-3 and RPE50%-3 were low DM pectins. And the DM values of

Table 2
The monosaccharide composition, molecular weight (M_w) and recovery rate of RPA50% fractions and RPE50% fractions.

	Monosaccharide compositions (mol%)							M_w (KDa)	Recovery rate (%)	Purity (%)
	Arabinose	Galactose	Rhamnose	Galacturonic acid	Xylose	Glucose	Mannose			
RPA50%-1	10.03 ± 0.66	15.01 ± 1.00	2.29 ± 0.08	4.82 ± 1.33	4.46 ± 0.18	57.93 ± 0.87	5.31 ± 0.04	2650 ± 1.50	5.01 ± 0.4	100
RPA50%-2	12.82 ± 3.16	28.53 ± 0.92	5.39 ± 0.21	17.99 ± 0.98	7.71 ± 1.86	27.63 ± 2.96	–	182 ± 1.11	7.36 ± 0.3	98.5
RPA50%-3	5.31 ± 0.17	14.45 ± 0.05	6.18 ± 0.17	65.59 ± 0.94	4.76 ± 0.03	3.73 ± 1.33	–	77 ± 3.26	25.44 ± 1.21	96.7
RPE50%-1	10.48 ± 2.00	10.00 ± 1.11	1.15 ± 1.14	2.42 ± 2.41	4.09 ± 0.54	65.38 ± 0.81	5.52 ± 0.21	1950 ± 0.93	5 ± 1.01	100
RPE50%-2	12.07 ± 0.31	20.07 ± 1.22	5.53 ± 0.09	14.17 ± 0.18	6.63 ± 1.4	34.03 ± 1.7	6.36 ± 1.64	71 ± 1.61	8 ± 0.76	92.7
RPE50%-3	16.40 ± 0.49	18.29 ± 0.24	4.93 ± 0.1	55.11 ± 0.15	0.53 ± 0.5	0.78 ± 0.29	0.71 ± 0.07	51 ± 0.48	42 ± 1.43	94.3
RPE50%-4	3.97 ± 0.44	2.51 ± 0.46	1.48 ± 0.77	91.25 ± 2.48	–	–	–	50 ~ 6	6 ± 2.19	65.7

Values represent means ± standard derivatives of three replicates;
- indicated not detected.

RPA50%-3 and RPE50%-3 were determined as 36% and 39% by HPLC method (Fig. S5), respectively.

3.3. Analysis of anti-inflammatory activities of RPA50%-3 and RPE50%-3

The biological activity of RPA50%-3 and RPE50%-3 has been determined based on murine macrophage RAW264.7 cells. Macrophages are one of the most abundant immune cells and play an important role in a variety of biological processes, including initiating inflammation (Sisirak et al., 2016; Smith et al., 2011). Bacterial LPS can stimulate and activate macrophages via the cell membrane receptor CD14 and, thus, induce much higher amount of inflammatory molecules than in normal conditions, such as inflammatory cytokines (TNF-α, IL-6 and IL-1β) and NO. The considerable accumulation of these molecules will exacerbate the inflammatory response. Additionally, there is high production of ROS during the inflammatory response, leading to DNA damage and cell death (Fubini & Hubbard. 2003). Therefore, reducing the level of inflammatory cytokines, NO and ROS could alleviate inflammation and the production changes on LPS-induced macrophages can be employed to evaluate the anti-inflammatory activity of pectins. In the present study, we determined the effects of RPA50%-3 and RPE50%-3 on the cell viability of normal RAW264.7 by CCK8 kit. These dosages of the two pectins exhibited cell growth above 97%, suggesting that these pectins had no cytotoxicity on macrophages (Fig. 2A). After being stimulated by LPS, the NO production of RAW264.7 cells increased about 4-fold (Fig. 2B). Both of these pectins could significantly reduce the level of NO in a dose-dependent manner. Moreover, RPE50%-3 showed better effects than RPA50%-3 with significant differences at the concentration of 200 μg/mL. Moreover, the changes on cytokines production could be observed at the dose of 200 μg/mL. The treatment of LPS on RAW264.7 could significantly increase the production of pro-inflammatory cytokines TNF-α, IL-6 and IL-1β by 183%, 286% and 83%, respectively. Both of RAP50%-3 and REP50%-3 could remarkably decrease the level of IL-1β (Fig. 2F). Compared to the model group, REP50%-3 also significantly declined the concentration of TNF-α and IL-6, while there were no significant differences in the RAP50%-3 group. These results indicated that more neutral sidechains in RG-I pectin might help the inhibition of inflammation responses, which was in accordance with previous work (Wu et al., 2021b; Ishisono et al., 2019). Also, both RPA50%-3 and RPE50%-3 alleviated the ROS production in LPS-treated macrophages, and RPE50%-3 exhibited better protective effects against oxidative stress (Fig. 2C). It has been reported that raspberry polysaccharides can reduce the intracellular ROS level (Chen et al., 2020). Ultrasound-assisted modified pectin showed higher bioactivity than raspberry pectin. However, the important structural factors remained unclear. Our results revealed that both RPA50%-3 and RPE50%-3 were low-esterified pectin with the molecular weight of 50 ~ 80 KDa, while RPE50%-3 contained more arabinan sidechains. Based on the cell culture assay, RPE50%-3 showed better anti-inflammatory properties, suggesting that arabinan sidechains could contribute to the anti-inflammatory activity of biological pectin.

The mechanism by which pectin exhibited the anti-inflammatory effects might be through the interaction of pectin and TLR receptors in the surface of immune cells. The non-esterified GalA in pectin could bind to TLR2 and inhibit proinflammatory TLR2-TLR1 pathway (Sahasrabudhe et al., 2018). This might be the reason why both of RPA50%-3 and RPE50%-3 are anti-inflammatory. Moreover, an arabinan-rich pectin has been reported to be immunobiological on the murine lymphocyte (Dourado et al., 2004). Likewise, arabinan from *Ligusticum chuanxiong* could regulate the production of inflammatory cytokines in RAW264.7 cell (Zhang et al., 2021). Previous studies suggested that arabinan possessed excellent immunomodulatory activity, and REP50%-3 exhibited better effects could be due to higher amount of arabinan sidechains than RAP50%-3. However, the potential mechanism by which arabinan sidechains function need further exploration.

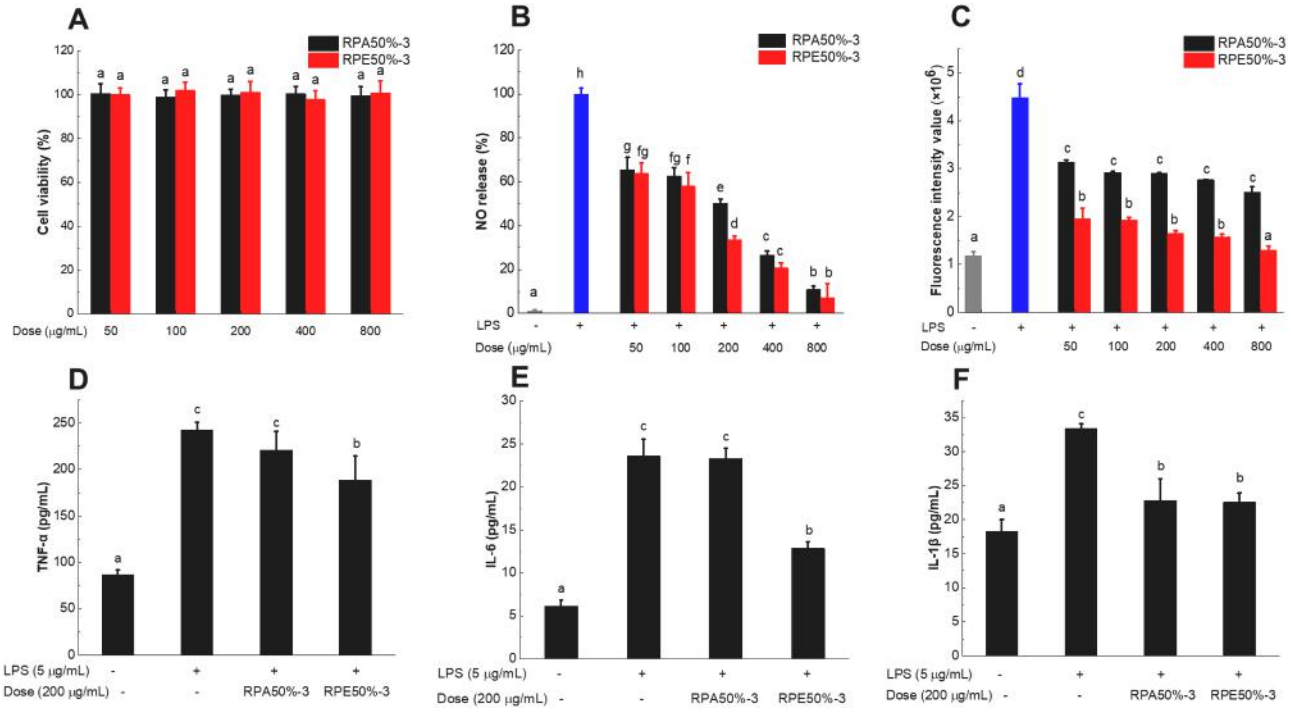

Fig. 2. The effects of RPA50%-3 and RPE50%-3 on RAW264.7 cell line: (A) Cytotoxicity of the two pectins on RAW264.7 cell (B) Effects of the two pectins on NO release by LPS-induced RAW264.7 cell (C) Effects of the two pectins on the intracellular ROS levels of LPS-induced RAW264.7 (D) Effects of the two pectins on TNF-α production of LPS-induced RAW264.7 (E) Effects of the two pectins on IL-6 production of LPS-induced RAW264.7 (F) Effects of the two pectins on IL-1β production of LPS-induced RAW264.7. Groups with different letters are significantly different ($p < 0.05$).

3.4. Structural characterization of RPE50%-3

The two pectin samples had similar chemical structure features and RPE50%-3 contained more complete sidechains regions and the cell culture assays revealed RPE50%-3 possessed better immunomodulatory effects. Therefore, RPE50%-3 was applied for further structural elucidation study.

One-dimension (1D) and two-dimension (2D) NMR spectroscopy, including ^{1}H, ^{13}C, ^{1}H–^{1}H COSY, ^{1}H–^{13}C HSQC and ^{1}H–^{13}C HMBC, were applied to reveal the precise structure of RPE50%-3 further. The primary chemical shifts of these residues are listed in Table S1.

In the ^{1}H NMR spectrum of RPE50%-3 (Fig. 3A), signal δ 5.01 could be assigned to the H-1 of 1,4-linked α-GalA, and the signal at δ 4.88 was attributed to the methyl-esterified GalA (Li et al., 2019). The signals at δ 5.08 and δ 4.99 were assigned to H-1 of 1,3-linked α-Ara*f* and 1.5-linked α-Ara*f*, respectively. The signal of H-1 of α-1,3,5-Ara was overlapped, which were confirmed by the cross-peak at 5.05/109.24 ppm in the HSQC spectrum (Fig. 4B). Resonance at δ 5.22 was attributed to the H-1 of Rha residues (B and C). Signals at δ 4.51 and δ 4.55 were assigned to 1,4-linked β-Gal*p* and 1, 6-linked β-Gal*p*, respectively. The peak signal at δ 3.71 was attributed to –OCH_3 chemical group. In the anomeric region of the ^{1}H–^{1}H COSY spectrum of RPE50%-3 (Fig. 4A), the intensive correlation peak of H^1/H^2 (5.01/4.28) was attributed to α-1,4-linked GalA residues. The presence of GalA-OMe could be confirmed by the cross-peak of H^1/H^2 (4.88/4.13). The correlation peaks at 5.08/4.38 ppm, 5.05/4.37 ppm, 4.99/4.31 ppm, 4.50/3.43 ppm, 5.22/3.75 ppm were assigned to the H^1/H^2 of α-1,3-Ara*f*, α-1,3,5-Ara*f*, α-1,5-Ara*f*, β-1,4-Gal*p* or β-1,6-Gal*p*, α-1,2,4-Rha*p* or α-1,2-Rha*p*, respectively. In the anomeric region of the ^{13}C NMR spectrum of RPE50%-3 (Fig. 3B), the intense anomeric signals around δ 110 - δ 109.24 could be attributed to C-1 of α-Ara*f* (D, E, and F). Signals at 105–106 ppm could be assigned to the anomeric carbon of different β-Gal*p* residues (G and H). The C-1 of α-1,4-GalA could be observed by the intensive signal at δ 101.91. The signal of methyl-esterified GalA (GalA-OMe) was assigned to δ 102.31, which could be confirmed by the intensive cross-peak at 4.88/102.31 ppm in the HSQC spectrum (Li et al., 2019). Also, the correlation peak at 3.71/56 ppm in HSQC spectrum was assigned to –OCH3 chemical group. The small peak at δ 96.22 was from the C-1 of α-Rha*p* residues (B and C) (Feng, Du, & Wang, 2021; Dutton, Merrifield, Laffite, Pratviel-Sosa, & Wylde, 1982). The weak signal at δ 19.50 was assigned to –CH_3 from Rha residues.

Combined analysis of COSY and HSQC spectra (Fig. 4A and B) allowed signals from different residues to be assigned. The anomeric region of the HSQC spectrum contained an intensive signal H^1/C^1 of α-1,4-GalA at 5.01/101.91 ppm, suggesting the major homogalacturonan of RPE50%-3. Additionally, some correlation peaks at C^2/H^2 (4.23/70.35 ppm), C^3/H^3 (3.94/71.81 ppm), and C^6 (δ 179 and δ 171) could be assigned to α-1,4-GalA (Kostalova & Hromadkova 2019; Zhou et al., 2018). The 5.22/96.22 ppm could be assigned to the α-1,2-Rha*p* and the substituted 1,2,4-α-Rha*p*. The α-Ara residues could be identified with characteristic H^1/C^1 at 5.08/109.55 ppm (α-1,3-Ara*f*), 5.05/109.24 ppm (α-1,3,5-Ara*f*), 4.99/110.00 ppm (α-1,5-Ara*f*), respectively. The anomeric cross-peaks at 4.51/105.71 ppm and 4.55/105.70 ppm could be attributed to β-1,4-Gal*p* and β-1,6-Gal*p*, respectively (Xu, Qi, Goff, & Cui, 2020). Other chemical shifts were provided in Table S1.

HMBC spectrum was used to reveal the intra-connections between neighboring residues in RPE50%-3. As shown in Fig. 4C, the strong correlation in HMBC between H-4 (4.65 ppm) and C-1 (101.91 ppm) of residue A, C-3 (71.81 ppm) of A and H-1 (5.01 ppm) of A, confirmed the …→4)-α-GalpA-(1 → 4)-α-GalpA-(1→… backbone. The H-2 (4.23 ppm) of residue C and C-1 (101.45 ppm) of residue A, the C-1 (96.22 ppm) of residue B and H-3 (3.94 ppm) of residue A, indicated the existence of rhamnogalacturonan I backbone. The correlation peak between C-3 (86.32 ppm) and H-1 (5.08 ppm) of residue D revealed the sidechains of → 3)-α-Ara*f*-(1 → 3)-α-Ara*f*-(1 → . The correction between C-4 (81.55 ppm) and H-1 (4.99 ppm) of residue F, C-5 (76.58 ppm) and H-1 (4.99 ppm) of residue F, C-3 (73.21 ppm) and H-1 (4.99 ppm) of residue F indicated that the presence of sidechains → 5)-α-Ara*f*-(1 → 5)-α-Ara*f*-(1 → . The correction between C-5 (84.32 ppm) of α-1,3,5-Ara*f* and H-1 (4.99 ppm) of α-1,5-Ara*f*, C-3 (73.21 ppm) of α-1,5-Ara*f* and H-1 (5.05 ppm) of α-1,3,5-Ara*f*, confirmed that α-1,5-arabinan was partly branched. The H-1 signal (4.99 ppm) of α-1,5-Ara*f* had a correlation with C-3 (72.3 ppm) of β-1,4-Gal*p*, revealing the existence of arabinogalactan sidechain. Additionally, the intensive cross peak between C-3 (70.54 ppm) of α-1,2,4-Rha*p* and the H-2 (4.31 ppm) of α-1,5-Ara*f* confirmed that α-1,5-arabinan sidechain was linked to the O-4 of Rha residues. The correlation between C-2 (73.58 ppm) and H-4 (4.16 ppm) of β-1,4-Gal*p* showed the fragment of → 4)-β-Gal*p*-(1 → 4)-β-Gal*p*-(1 → . The cross peaks between C-6 (64.12 ppm) and H-2 (3.43 ppm), C-6 (64.12 ppm) and H-3 (3.75 ppm) of β-1,6-Gal*p* revealed the structure of β-1,6-Galactan.

As described above, the structure of RPE50%-3 is a highly branched pectin consisting of 50% of linear homogalacturonan, short RG backbone, 16.4% of long and branched α-1,5-arabinan and α-1,3-arabinan, 18.3% of β-1,4-galactan and β-1,6-galactan sidechains and minor arabinogalactan. The RG-I amount of RPE50%-3 was 44.55% and the Rha/GalA was calculated to be 0.09. Therefore, RPE50%-3 could be categorized as RG-I type pectin (Zhang et al., 2016).

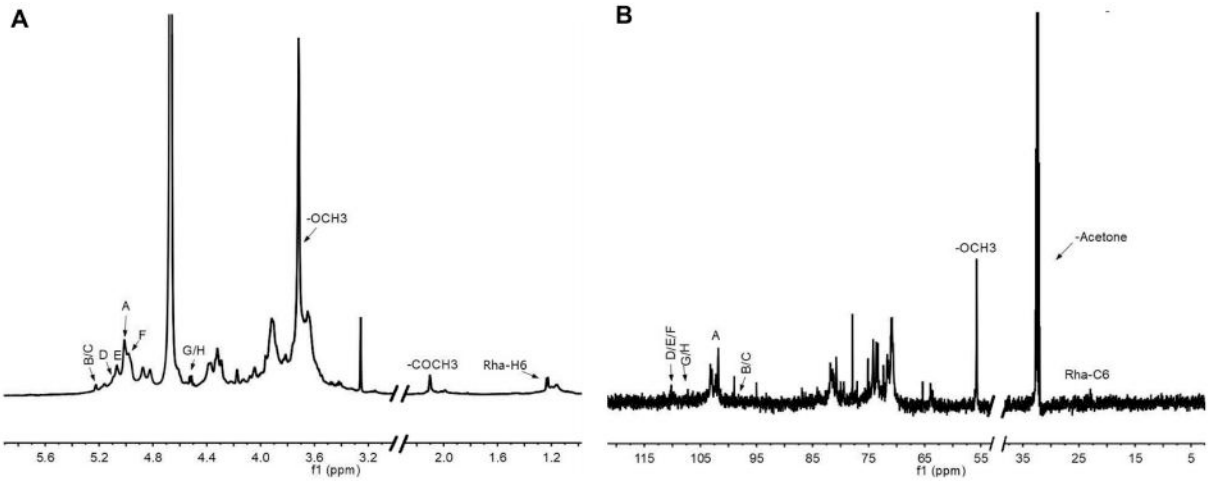

Fig. 3. 1D NMR spectra of RPE50%-3: ^{1}H (A) spectrum and ^{13}C (B) NMR spectrum.

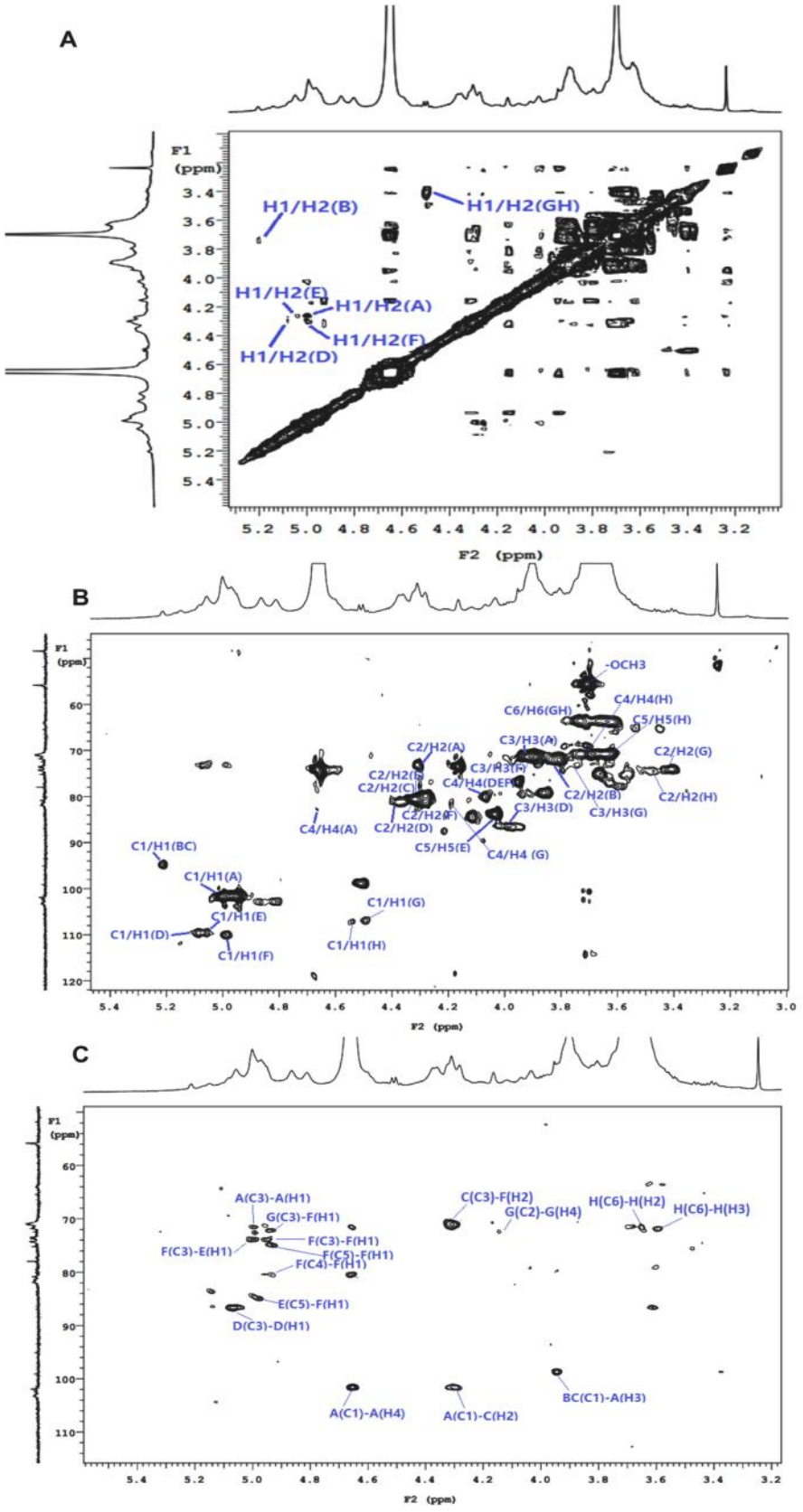

Fig. 4. 2D NMR spectra of RPE50%-3: $^{1}H/^{1}H$ COSY (A); $^{1}H/^{13}C$ HSQC (B) and $^{1}H/^{13}C$ HMBC (C) spectra.

4. Conclusions

In summary, crude raspberry polysaccharides were extracted from raspberry fruit by hot-acid and combined-enzymes methods. After stepwise ethanol precipitation and Q-fast flow column chromatography isolation, two purified pectins (RPA50%-3 and RPE50%-3) were obtained. Although, these two extraction methods had no remarkable effects on the molecular weight and degree of methylation, but enzyme-extracted raspberry pectin (RPE50%-3) contained a higher amount of arabinose, suggesting vigorous hot-acid extraction induced degradation of neutral sidechains in raspberry pectin. The structural characterization results suggested RPE50%-3 was RG-I pectin containing α-1,5-arabinan, α-1,3-arabinan, β-1,4-galactan, β-1,6-galactan and minor arabinogalactan sidechains. Besides, RPE50%-3 exhibited better immunomodulatory properties on lipopolysaccharides-activated macrophages. These results revealed that arabinan sidechains contributed to the regulation of pectin on immune cells. The enzyme-extraction method could keep the highly branched sidechains of raspberry pectin, and the traditional acidic extraction might not be suitable for producing bioactive pectin. This study provided fine structural information of pure raspberry pectin and also was helpful for rethinking efficient extraction of functional pectin in the food industry.

CRediT authorship contribution statement

Dongmei Wu: Data curation, Formal analysis, Investigation, Project administration, Writing – original draft. **Shiguo Chen:** Methodology, Funding acquisition, Writing – review & editing. **Xingqian Ye:** Funding acquisition, Writing – review & editing. **Xiaoliang Zheng:** Methodology. **Shokouh Ahmadi:** Methodology. **Weiwei Hu:** Supervision. **Chengxiao Yu:** Methodology. **Huan Cheng:** Resources. **Robert J. Linhardt:** Writing – review & editing. **Jianle Chen:** Resources, Methodology, Writing – review & editing.

Declaration of Competing Interest

The authors declare that they have no known competing financial interests or personal relationships that could have appeared to influence the work reported in this paper.

Acknowledgments

This work was supported by National Key Research and Development program of China (2017YFE0122300). In addition, we are grateful to Dr. Yaqin Liu (Department of Chemistry, Zhejiang University) for efficient NMR measurements.

Appendix A. Supplementary data

Supplementary data to this article can be found online at https://doi.org/10.1016/j.foodchem.2022.132387.

References

Chen, J., Cheng, H., Zhi, Z., Zhang, H., Linhardt, R. J., Zhang, F., … Ye, X. (2021). Extraction temperature is a decisive factor for the properties of pectin. *Food Hydrocolloids, 112*, 106160.

Chen, Y., Wang, Y., Xu, L., Jia, Y., Xue, Z., Zhang, M., … Chen, H. (2020). Ultrasound-assisted modified pectin from unripe fruit pomace of raspberry (*Rubus chingii Hu*): Structural characterization and antioxidant activities. *LWT-Food Science and Technology, 134*, 110007.

Cui, J., Ren, W., Zhao, C., Gao, W., Tian, G., Bao, Y., … Zheng, J. (2020). The structure-property relationships of acid- and alkali-extracted grapefruit peel pectins. *Carbohydrate Polymers, 229*, 115524.

Cosgrove, D. J. (2014). Re-constructing our models of cellulose and primary cell wall assembly. *Current Opinion in Plant Biology, 22*, 122–131.

Dourado, F., Madureira, P., Carvalho, V., Coelho, R., Coimbra, M. A., Vilanova, M., Mota, M., & Gama, F. M. (2004). Purification, structure and immunobiological activity of an arabinan-rich pectic polysaccharide from the cell walls of *Prunus dulcis* seeds. *Carbohydrate Research, 339*(15), 2555–2566.

Dutton, G. G. S., Merrifield, E. H., Laffite, C., Pratviel-Sosa, F., & Wylde, R. (1982). Comparative NMR Study of Rhamnobioses- Applications. *Organic Magnetic Resonance, 20*(3), 154–158.

Fan, L., Zuo, S., Tan, H., Hu, J., Cheng, J., Wu, Q., & Nie, S. (2020). Preventive effects of pectin with various degrees of esterification on ulcerative colitis in mice. *Food & Function, 11*, 2886–2897.

Feng, X., Du, C., & Wang, C. (2021). Structural characterization of polysaccharide from yellow sweet potato and ameliorates DSS-induced mice colitis by active GPR41/MEK/ERK 1/2 signaling pathway. *International Journal of Biological Macromolecules, 192*, 278–288.

Fubini, B., & Hubbard, A. (2003). Reactive oxygen species (ROS) and reactive nitrogen species (RNS) generation by silica in inflammation and fibrosis. *Free Radical Biology and Medicine, 34*(12), 1507–1516.

Gu, J., & Catchmark, J. M. (2013). The impact of cellulose structure on binding interactions with hemicellulose and pectin. *Cellulose, 20*(4), 1613–1627.

Guo, X., Meng, H., Zhu, S., Tang, Q., Pan, R., & Yu, S. (2016). Stepwise ethanolic precipitation of sugar beet pectins from the acidic extract. *Carbohydrate Polymers, 136*, 316–321.

Hu, W., Ye, X., Chantapakul, T., Chen, S., & Zheng, J. (2020). Manosonication extraction of RG-I pectic polysaccharides from citrus waste: Optimization and kinetics analysis. *Carbohydrate Polymers, 235*, 115982.

Hu, X., & Goff, H. D. (2018). Fractionation of polysaccharides by gradient non-solvent precipitation: A review. *Trends in Food Science & Technology, 81*, 108–115.

Ishisono, K., Mano, T., Yabe, T., & Kitaguchi, K. (2019). Dietary Fiber Pectin Ameliorates Experimental Colitis in a Neutral Sugar Side Chain-Dependent Manner. *Frontiers in Immunology, 10*, 2979.

Kazemi, M., Khodaiyan, F., & Hosseini, S. S. (2019). Eggplant peel as a high potential source of high methylated pectin: Ultrasonic extraction optimization and characterization. *LWT-Food Science and Technology, 105*, 182–189.

Kurita, O., Fujiwara, T., & Yamazaki, E. (2008). Characterization of the pectin extracted from citrus peel in the presence of citric acid. *Carbohydrate Polymers, 74*(3), 725–730.

Kostalova, Z., & Hromadkova, Z. (2019). Structural characterisation of polysaccharides from roasted hazelnut skins. *Food Chemistry, 286*, 179–184.

Laroze, L., Soto, C., & Zúñiga, M. E. (2010). Phenolic antioxidants extraction from raspberry wastes assisted by-enzymes. *Electronic Journal of Biotechnology, 13*(6), 1–12.

Levigne, S., Thomas, M., Ralet, M. C., Quemener, B., & Thibault, J. F. (2002). Determination of the degrees of methylation and acetylation of pectins using a C18 column and internal standards. *Food Hydrocolloids, 16*(6), 547–550.

Liu, X., Le Bourvellec, C., & Renard, C. (2020). Interactions between cell wall polysaccharides and polyphenols: Effect of molecular internal structure. *Comprehensive Reviews in Food Science and Food Safety, 19*(6), 3574–3617.

Liu, S., Yang, Y., Qu, Y., Guo, X., Yang, X., Cui, X., & Wang, C. (2020). Structural characterization of a novel polysaccharide from Panax notoginseng residue and its immunomodulatory activity on bone marrow dendritic cells. *International Journal of Biological Macromolecules, 161*, 797–809.

Li, K., Zhu, L., Li, H., Zhu, Y., Pan, C., Gao, X., & Liu, W. (2019). Structural characterization and rheological properties of a pectin with anti-constipation activity from the roots of *Arctium lappa L*. *Carbohydrate Polymers, 215*, 119–129.

Mao, G., Wu, D., Wei, C., Tao, W., Ye, X., Linhardt, R. J., … Chen, S. (2019). Reconsidering conventional and innovative methods for pectin extraction from fruit and vegetable waste: Targeting rhamnogalacturonan I. *Trends in Food Science & Technology, 94*, 65–78.

Milošević, M. M., & Antov, M. G. (2022). Pectin from butternut squash (*Cucurbita moschata*) -The effect of enzyme-assisted extractions on fiber characteristics and properties. *Food Hydrocolloids, 123*, 107201.

Mohnen, D. (2008). Pectin structure and biosynthesis. *Current Opinion in Plant Biology, 11*(3), 266–277.

Mzoughi, Z., Abdelhamid, A., Rihouey, C., Le Cerf, D., Bouraoui, A., & Majdoub, H. (2018). Optimized extraction of pectin-like polysaccharide from *Suaeda fruticosa* leaves: Characterization, antioxidant, anti-inflammatory and analgesic activities. *Carbohydrate Polymers, 185*, 127–137.

Saberian, H., Hamidi-Esfahani, Z., Ahmadi Gavlighi, H., & Barzegar, M. (2017). Optimization of pectin extraction from orange juice waste assisted by ohmic heating. *Chemical Engineering and Processing: Process Intensification, 117*, 154–161.

Sahasrabudhe, N. M., Beukema, M., Tian, L., Troost, B., Scholte, J., Bruininx, E., … de Vos, P. (2018). Dietary Fiber Pectin Directly Blocks Toll-Like Receptor 2–1 and Prevents Doxorubicin-Induced Ileitis. *Frontiers in Immunology, 9*, 1–15.

Shivamathi, C. S., Gunaseelan, S., Soosai, M. R., Vignesh, N. S., Varalakshmi, P., Kumar, R. S., … Ganesh Moorthy, I. M. (2022). Process optimization and characterization of pectin derived from underexploited pineapple peel biowaste as a value-added product. *Food Hydrocolloids, 123*, 107141.

Smith, P. D., Smythies, L. E., Shen, R., Greenwell-Wild, T., Gliozzi, M., & Wahl, S. M. (2011). Intestinal macrophages and response to microbial encroachment. *Mucosal Immunology, 4*(1), 31–42.

Sisirak, V., Sally, B., D'Agati, V., Martinez-Ortiz, W., Ozcakar, Z. B., David, J., … Reizis, B. (2016). Digestion of Chromatin in Apoptotic Cell Microparticles Prevents Autoimmunity. *Cell, 166*(1), 88–101.

Soria, A. C., Corzo-Martínez, M., Montilla, A., Riera, E., Gamboa-Santos, J., & Villamiel, M. (2010). Chemical and physicochemical quality parameters in carrots dehydrated by power ultrasound. *Journal of Agricultural and Food Chemistry, 58*, 7715–7722.

Szymanska-Chargot, M., & Zdunek, A. (2013). Use of FT-IR Spectra and PCA to the Bulk Characterization of Cell Wall Residues of Fruits and Vegetables Along a Fraction Process. *Food Biophysics, 8*(1), 29–42.

Tian, W., Yang, Y., Wu, Y., & Chen, W. (2020). Immune regulation and antioxidant activity of raspberry pulp polysaccharide through type 1 diabetic rats. *Food and Fermentation Industries, 46*, 102–108.

Voragen, A. G. J., Coenen, G. J., Verhoef, R. P., & Schols, H. A. (2009). Pectin, a versatile polysaccharide present in plant cell walls. *Structural Chemistry, 20*, 263–275.

Vriesmann, L. C., & de Oliveira Petkowicz, C. L. (2009). Polysaccharides from the pulp of cupuassu (*Theobroma grandiflorum*): Structural characterization of a pectic fraction. *Carbohydrate Polymers, 77*(1), 72–79.

Wang, L., Liu, H. M., & Qin, G. Y. (2017). Structure characterization and antioxidant activity of polysaccharides from Chinese quince seed meal. *Food Chemistry, 234*, 314–322.

Wei, C., Zhang, Y., He, L., Cheng, J., Li, J., Tao, W., … Chen, S. (2019). Structural characterization and anti-proliferative activities of partially degraded polysaccharides from peach gum. *Carbohydrate Polymers, 203*, 193–202.

Wu, D., Chen, S., Ye, X., Ahmadi, S., Hu, W., Yu, C., … He, Q. (2021a). Protective effects of six different pectic polysaccharides on DSS-induced IBD in mice. *Food Hydrocolloids, 107209*.

Wu, D., Zheng, X., Hu, W., Zhu, K., Yu, C., He, Q., … Chen, S. (2021b). Anti-inflammation effects of highly purified low-Mw RG-I pectins on LPS-activated macrophages. *Bioactive Carbohydrates and Dietary Fibre, 26*, 100283.

Wu, D., Ye, X., Linhardt, R. J., Liu, X., Zhu, K., Yu, C., … Chen, S. (2021c). Dietary pectic substances enhance gut health by its polycomponent: A review. *Comprehensive Reviews in Food Science and Food Safety, 20*(2), 2015–2039.

Wu, D., Zheng, J., Mao, G., Hu, W., Ye, X., Linhardt, R. J., … Chen, S. (2020a). Rethinking the Impact of RG-I Mainly from Fruits and Vegetables on Dietary Health. *Critical Reviews in Food Science and Nutrition, 60*(17), 2938–2960.

Wu, D., Zheng, J., Hu, W., Zheng, X., He, Q., Linhardt, R. J., … Chen, S. (2020b). Structure-activity relationship of citrus segment membrane RG-I pectin against Galectin-3: The galactan is not the only important factor. *Carbohydrate Polymers, 245*, 116526.

Xu, M., Qi, M., Goff, H. D., & Cui, S. W. (2020). Polysaccharides from sunflower stalk pith: Chemical, structural and functional characterization. *Food Hydrocolloids, 100*, 105082.

Xu, Y., Liu, N., Fu, X., Wang, L., Yang, Y., Ren, Y., … Wang, L. (2019). Structural characteristics, biological, rheological and thermal properties of the polysaccharide and the degraded polysaccharide from raspberry fruits. *International Journal of Biological Macromolecules, 132*, 109–118.

Yang, J., Wen, L., Zhao, Y., Jiang, Y., Tian, M., Liu, H., … Yang, B. (2018). Structure identification of an arabinogalacturonan in *Citrus reticulata Blanco 'Chachiensis'* peel. *Food Hydrocolloids, 84*, 481–488.

Yang, Y. J., Xu, H. M., & Suo, Y. R. (2015). Raspberry pulp polysaccharides inhibit tumor growth via immunopotentiation and enhance docetaxel chemotherapy against malignant melanoma in vivo. *Food & Function, 6*(9), 3022–3034.

Yu, Z., Liu, L., Xu, Y., Wang, L., Teng, X., Li, X., & Dai, J. (2015). Characterization and biological activities of a novel polysaccharide isolated from raspberry (*Rubus idaeus L.*) fruits. *Carbohydrate Polymers, 132*, 180–186.

Zhang, S., An, L., Li, Z., Wang, X., Wang, H., Shi, L., … Guo, Y. (2021). Structural elucidation of an immunological arabinan from the rhizomes of *Ligusticum chuanxiong*, a traditional Chinese medicine. *International Journal of Biological Macromolecules, 170*, 42–52.

Zhang, H., Chen, J., Li, J., Yan, L., Li, S., Ye, X., … Chen, S. (2018). Extraction and characterization of RG-I enriched pectic polysaccharides from mandarin citrus peel. *Food Hydrocolloids, 79*, 579–586.

Zhang, T., Lan, Y., Zheng, Y., Liu, F., Zhao, D., Mayo, K. H., … Tai, G. (2016). Identification of the bioactive components from pH-modified citrus pectin and their inhibitory effects on galectin-3 function. *Food Hydrocolloids, 58*, 113–119.

Zhou, L., Liao, W., Zeng, H., Yao, Y., Chen, X., & Ding, K. (2018). A pectin from fruits of *Lycium barbarum L.* decreases beta-amyloid peptide production through modulating APP processing. *Carbohydrate Polymers, 201*, 65–74.

Zykwinska, A. W., Ralet, M. C., Garnier, C. D., & Thibault, J. F. (2005). Evidence for *in vitro* binding of pectin side chains to cellulose. *Plant Physiology, 139*(1), 397–407.